Building and Environment, Vol. 22, No. 4, pp. 293–304, 1987.
Printed in Great Britain.

0360–1323/87 $3.00 + 0.00

Air Flow Through Cracks

P. H. BAKER*
S. SHARPLES*
I. C. WARD*

The pressure flow characteristics of a number of full-scale model cracks, representative of real leakage paths, have been measured. The crack flow equations developed by Etheridge [1] *have been verified over a wider range of parameters. The authors suggest a quadratic relationship:*

$$\Delta P = A \cdot Q + B \cdot Q^2$$

which follows from the same flow theory as the Etheridge solution, to replace the ubiquitous power law as a practical fit to pressurisation data. Unlike the power law, the quadratic coefficients A and B can be directly related to crack parameters, and a simple graphical method is given to enable the prediction of crack leakage areas.

1. INTRODUCTION

1.1. *Crack flow equations*

Equations of the form

$$\Delta P = \alpha \cdot Q^{\beta} \tag{1}$$

have been widely used to describe the flow through cracks. It has been found that the power law can be used to describe the relationship between volume flow rate Q and pressure drop ΔP for a wide range of crack geometries. However, as Etheridge [1] points out, equations of this type lack generality because they are not dimensionally homogenous, that is they do not obey Reynolds law of similitude.

Some evidence [2, 3] suggests that the flow rate is approximately proportional to the square root of the pressure drop:

$$Q = a\sqrt{\Delta P} \tag{2}$$

where a is a constant proportional to the effective leakage area of the crack.

This simple law also applies to turbulent flow through a thin plate orifice, and so the area of the equivalent thin plate orifice to which the crack approximates may be calculated. However, in practice the relationship does not fit the available data. Hopkins and Hansford [4] give a number of reasons for this deviation from theory: (i) the open area increases as the pressure difference increases, due to distortion of the crack. (ii) The orifice plate equation used to estimate the leakage area assumes a constant value of the discharge coefficient; any variation in the discharge coefficient will produce a deviation from the theory. (iii) The square law approximation is not strictly true for all types of crack, crack geometries and pressure differences.

Thomas and Dick [5] found that for the pressurisation testing of windows the flow-pressure data fitted a curve of the form:

$$\Delta P = A \cdot Q + B \cdot Q^2 \tag{3}$$

and that there was some correlation between the constants A and B and the window gap dimensions.

Jones [6] and Etheridge [7] suggest that the above relationship might be used rather than the power law or the square law. Although the quadratic disregards the existence of a critical velocity of transition between streamline and turbulent flow, it has the practical advantage that at both extremes, i.e. $Q \to 0$ and $Q \to \infty$, it gives the correct forms corresponding respectively to laminar flow and to complete turbulence. The coefficients A and B remain independent of the rate of flow.

1.2. *Theoretical basis of the quadratic equation*

It can be shown that the use of the quadratic equation to describe the flow characteristics of simple components has some theoretical validity. The basic flow equation for laminar flow through infinite parallel plates [8] is:

$$\frac{Q}{L} = \frac{d^3 \Delta P_f}{12\mu z} \tag{4}$$

where ΔP_f is the pressure drop due to skin friction along the dimension z in the direction of flow, d is the gap thickness, L is the breadth of the plates and μ is the dynamic viscosity. Rearranging gives:

$$\Delta P_f = \frac{Q}{L}\frac{12\mu z}{d^3} \tag{5}$$

Now the total pressure drop allowing for edge effects, that is flow contraction and expansion pressure drops, is

$$\Delta P_{\text{TOTAL}} = \frac{Q}{L}\frac{12\mu z}{d^3} + C \cdot \frac{\rho}{2}\left(\frac{Q}{d \cdot L}\right)^2 \tag{6}$$

where C is a dimensionless constant, ρ is density.

It is clear that this equation reduces to

$$\Delta P_{\text{TOTAL}} = A \cdot Q + B \cdot Q^2 \tag{7}$$

where

$$A = 12\mu z / L d^3$$

*Department of Building Science, University of Sheffield, Sheffield S10 2TN, U.K.

and

$$B = \rho \cdot C/2d^2L^2.$$

It can also be shown that the quadratic is dimensionally homogenous.

Hopkins and Hansford [4] and Etheridge [1] have suggested an equation of the form

$$\frac{1}{C_d^2} = k\frac{z}{Re_h D_h} + C \tag{8}$$

where C_d is the discharge coefficient of the crack, Re_h is the Reynolds number based on the hydraulic diameter D_h, C is an empirical constant and k is an apparent coefficient which varies with Reynolds number and aspect ratio. The above relationship, like the quadratic, is also derived from the basic flow equation for steady laminar flow between infinite parallel plates (equation 4) with the addition of a term for edge effects; however its greater usefulness, certainly from a theoretical viewpoint, compared to the quadratic form is that the terms $1/C_d^2$ and z/Re_hD_h are non-dimensional. In practice, the quadratic may be more suitable for the estimation of leakage areas through components.

1.3. *Experimental crack flow measurements*

The validity of equation (8) has been tested by pressurisation testing of model cracks of the 'straight through', 'L-shaped' and 'multi-cornered' types [4]. Curves of the form of equation (8) were fitted to available data with some reservations for the L-shaped and multi-cornered cracks, where deviations from a smooth curve occur. These can be explained by flow separation effects at the bends in the model cracks, witnessed by flow visualisation by means of smoke. Values of the coefficients k and C were obtained for each crack, and then average values of these were calculated for each of the three types of crack to enable semi-empirical curves to be drawn through the data [Figs 1(a)–(c)]. These appear to give a good fit, regardless of the deviations.

Hopkins and Hansford suggest that the semi-empirical equations can be used to evaluate discharge coefficients for each type of crack to be used in conjunction with an orifice plate solution, of the form of equation (2). Etheridge [1] points out that such a combination is both inconsistent and unnecessary, since the flow is completely and rigorously described by equation (8) alone. Although equation (8) is a simplified representation of a complex flow situation, Etheridge found it successful for estimating both the open areas of real full-scale components and for describing the flow through them. Since it takes into account Reynolds number effects the estimated values of open area are independent of the flow rate through the open area. This also means that where an open area can in fact be obtained by direct measurement, the value can be used directly in the equation to estimate the leakage flow under a given pressure differential. Etheridge further noted that the empirical values of slope obtained for the straight-through and L-shaped cracks were close to a theoretical value of 96 derived from the equations for flow between parallel plates. This supports the assumption that the pressure drop can be considered as two additive components, i.e. due to skin friction and edge effects.

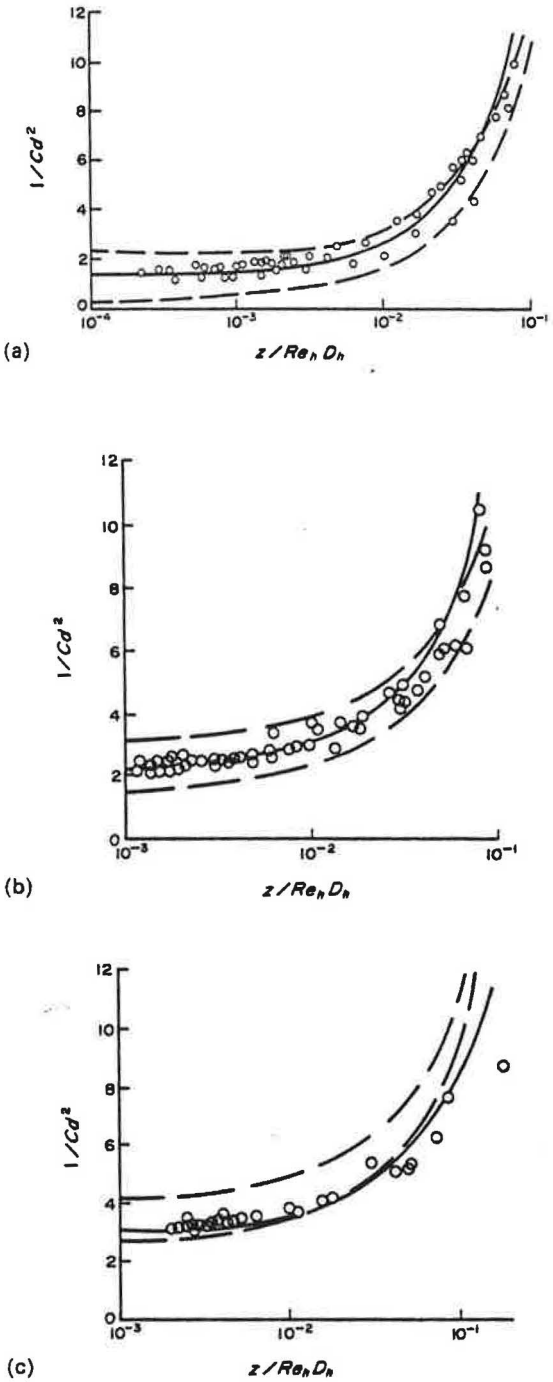

Fig. 1. Hopkins and Hansford's data showing their semi-empirical relationship (———), and the 95% prediction intervals for $1/Cd^2$ (– – – –) calculated for each crack type from the data in Figs 4–6. (a) Straight-through cracks, (b) L-shaped cracks, (c) double bend cracks.

In the present study, the experimental work of Hopkins and Hansford [4] has been extended over a wider range of Reynolds numbers, and the validity of equation (8) has been examined, particularly as a description for cracks with one or more bends. A quadratic analysis of crack flow has also been made as a simplified but still rigorous description.

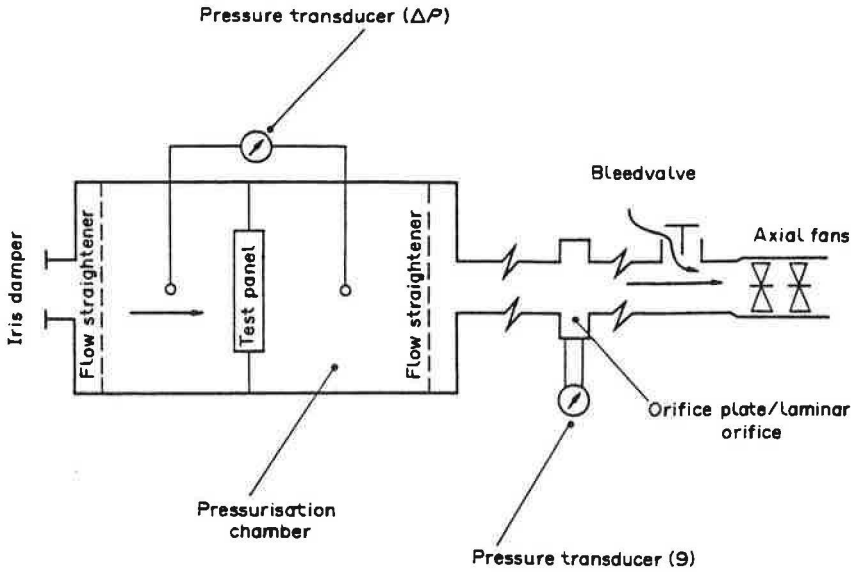

Fig. 2. Schematic diagram of test facility.

2. EXPERIMENTAL EQUIPMENT AND PROCEDURES

2.1. *Experimental apparatus*

The experimental arrangement is shown schematically in Fig. 2. Crack models, described below, were fitted into the detachable front of the pressurisation chamber, which was depressurised using a combination of a bleed valve and fans in series to produce a range of flow rates up to 0.01 m^3/s. The pressure difference across a crack was measured using either a pressure transducer or a micromanometer connected to two pressure tappings, one positioned centrally in the pressurisation chamber the other in the shield box, used as protection against external pressure fluctuations in the laboratory, e.g. doors closing. As the work progressed it was found that a simple sheltered pressure tapping sufficed without the need of the shield box.

Flow rates below 0.00167 m^3/s (100 l/min) were measured with a commercially available laminar flow orifice device. The pressure drop across this factory calibrated device is a linear measure of flow rate with 100 l/min = 1.90 mm H_2O. Flow rates above 0.00167 m^3/s were measured using an orifice plate constructed and calibrated according to BS 1042 [9]. Since the discharge coefficient of the orifice plate is dependent on flow rate, the final value of the discharge coefficient and hence of flow rate must be obtained by iteration from an initial chosen value of Reynolds number. The British Standard suggests $Re = 10^6$ as the starting point. The calibration was independently checked over a limited range of flows, 0.0019–0.0043 m^3/s, by attaching in series a smooth calibration pipe fitted with a micrometer traversing pitot [10]. The flows measured using both the orifice plate and a 10-point 'log-linear' pitot traverse [10, 11] agreed within 5%; thus the orifice plate calibration was accepted as satisfactory. Various pressure transducers were used during the measurements which enabled a wide span of pressure differentials across cracks to be measured, typically in the range 0.5–100 Pa with the available fan system.

2.2. *Experimental procedure*

The pressure drop across the crack was set up by adjusting the bleed valve of the fan system. When the pressure drop/flow readings had become steady the data were recorded for 2 min on a chart recorder or 500 scans per data pair were made with a data logging system. The procedure was then repeated over the required range of pressure drops. The crack was then sealed over, in order to measure the adventitious flows or 'leakage' of the pressurisation facility. Adventitious flow measurements were made at approximately the same pressure differences as the crack flow experiments. Since a rigorous analysis of the adventitious leakage data was not required, curves were fitted in the form:

$$Q_a = k_1 \Delta P^{k_2}$$

with excellent agreement (correlation coefficient $r > 0.98$ for all data fits).

Since the crack flow experiment actually gave the total flow (crack + adventitious) at pressure difference ΔP, the adventitious leakage flow Q_a was calculated at ΔP using the above relationship and then subtracted from the total flow to give the air flow through the crack. Whirling psychrometer measurements of dry and wet bulb temperatures were made, and barometric pressure taken, enabling air density to be estimated and air viscosity/kinematic viscosity to be calculated under ambient conditions.

The results of the experiments were generally treated by both the following methods: (i) the non-dimensional parameters $1/C_d^2$ and z/Re_hD_h were calculated, and plotted to obtain a relationship of the form

$$\frac{1}{C_d^2} = k\frac{z}{Re_hD_h} + C. \tag{8}$$

(ii) The flow–pressure drop data were fitted to a quadratic to obtain the coefficients A and B in equation (7). Theoretical values of A and B were also obtained by

using the relationships

$$A = 12\mu z/Ld^3, \tag{9}$$

$$B = \rho C/2d^2L^2 \tag{10}$$

and assuming values of the loss coefficient, C on the following basis: $C = 1.5$ for straight through cracks, $C = 2.5$ for L-shaped cracks, $C = 3.5$ for double bend crack etc., this follows from pipe flow experiments, where, for sudden contraction and expansion, the loss coefficients are 0.5 and 1.0 respectively, and for a sharp bend the loss coefficient is 1.0. These assumptions may not be true for rectangular cross-section cracks. The theoretical and measured values of A and B were then able to be compared.

3. FLOW THROUGH MODEL CRACKS

3.1. *Crack flow modelling*

Three basic types of crack have been examined which are representative of real leakage paths through, for example, doors and windows, and which may serve as models of background leakage paths: (i) Straight-through, (ii) L-shaped, i.e. one 90° bend, (iii) Multi-cornered, i.e. two or more 90° bends.

Initial measurements made on a 3.22 mm thick crack had suggested that the flow per unit length Q_L/L through a crack of length L was independent of crack length provided that the length is much greater than the crack thickness. Figure 3 shows Q_L/L plotted against ΔP and demonstrates the independence of the flow per unit length on crack length. Consequently, for convenience a standard crack length of 0.5 m was chosen for all measurements. Crack dimensions are given in Table 1.

The thickness of a crack was originally set using end spacers of known thickness. However, due to bowing of the ground flat steel plates used to fabricate the earliest 'straight-through' models, the average of feeler gauge measurements made over 21, 25 or 50 positions (depending on crack type) along the crack length were taken as a better estimate of crack thickness. The average standard deviation for the thickness of straight-through cracks was ±0.08 mm, and that for L-shaped and multi-cornered cracks ±0.09 mm. For 0.5 mm cracks these deviations are approximately 20%, which may be considered unacceptable, therefore, no attempt was made to fabricate thinner cracks. For ease of manufacture and cost the L-shaped and multi-cornered cracks were made from perspex sheet. Although this does not have the flatness of ground flat steel, its lightness and rigidity when made up into crack models produced good accuracy.

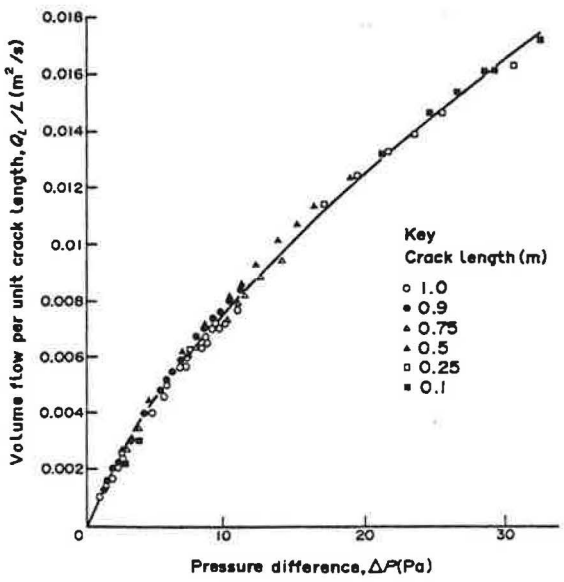

Fig. 3. Q_L/L vs ΔP for 3.22 mm crack.

Table 1. Crack types and dimensions

(i) Straight-through cracks

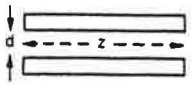

z mm	d mm
152	0.38, 0.90, 1.40, 3.05, 6.15, 9.40
76	0.55, 1.03, 1.39, 2.85, 5.85, 8.94
50	0.49, 1.17, 1.79, 3.20, 6.08, 9.13

(ii) L-shaped cracks

a mm	b mm	z mm	d mm
50	50	94.00	6.00
50	50	96.02	2.98
50	50	98.91	1.09
50	20	64.01	5.99
50	20	66.90	3.10
50	20	68.92	1.08

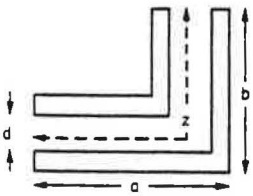

(iii) Multi-cornered cracks

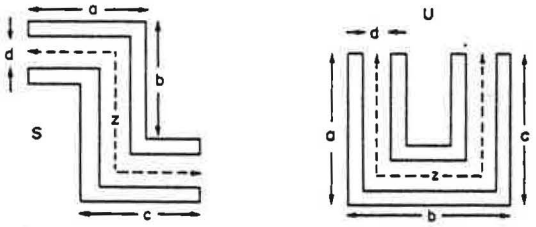

Type	a mm	b mm	c mm	z mm	d mm
S	50	50	50	150	3.16
S	50	50	50	150	1.09
S	20	20	50	60	3.14
S	20	20	20	60	1.09
U	50	50	50	143.53	3.23

4. RESULTS

4.1. *Non-dimensional parametric solution*

The non-dimensional parameters $1/C_d^2$ and z/Re_hD_h were calculated from the measured data for each crack type. Results are shown in Figs 4–6, where a logarithmic

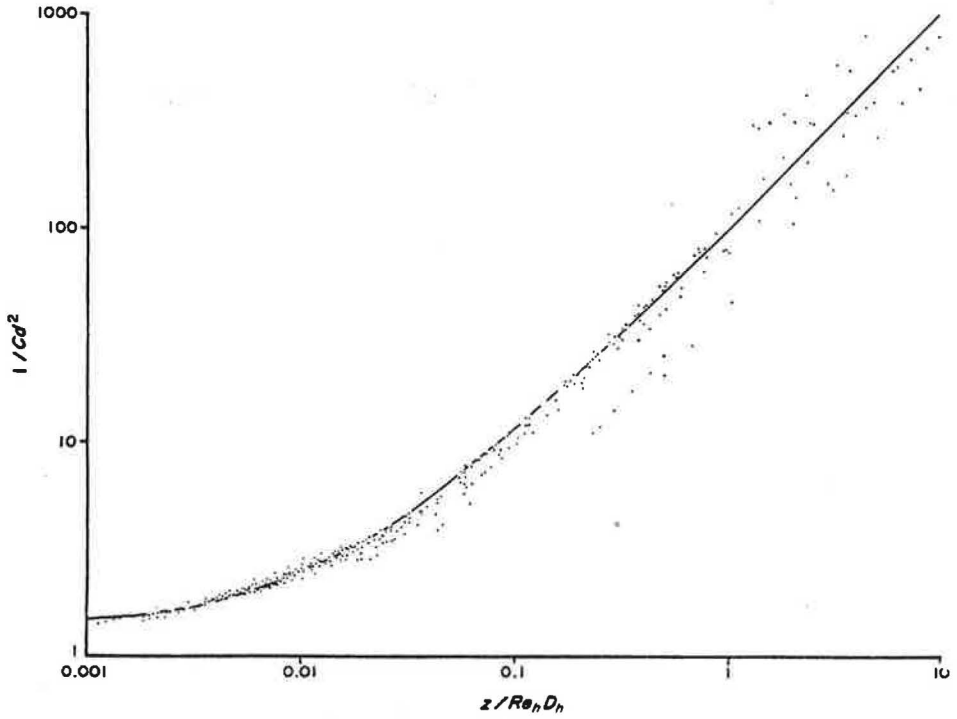

Fig. 4. The relationship between the non-dimensional parameters for flow through straight-through cracks.

scale has been chosen since the parameters range over 3 to 5 decades. The maximum value of z/Re_hD_h obtained in the present study is about 10 for each crack type. This compares to a range of 0.13–0.4 achieved by Hopkins and Hansford [4] for similar crack geometries. Figures 4–6 indicate, with the exception of data for some L-shaped cracks which showed dependence on flow direction [12], that the characteristics of each crack type can be described by a continuous function.

Etheridge [1] has shown that Hopkins and Hansford's data fitted linear relationships of the form of equation (8). On first examination, a linear fit using standard least squares linear regression proved to be inadequate. For example, for the straight-through cracks, least squares

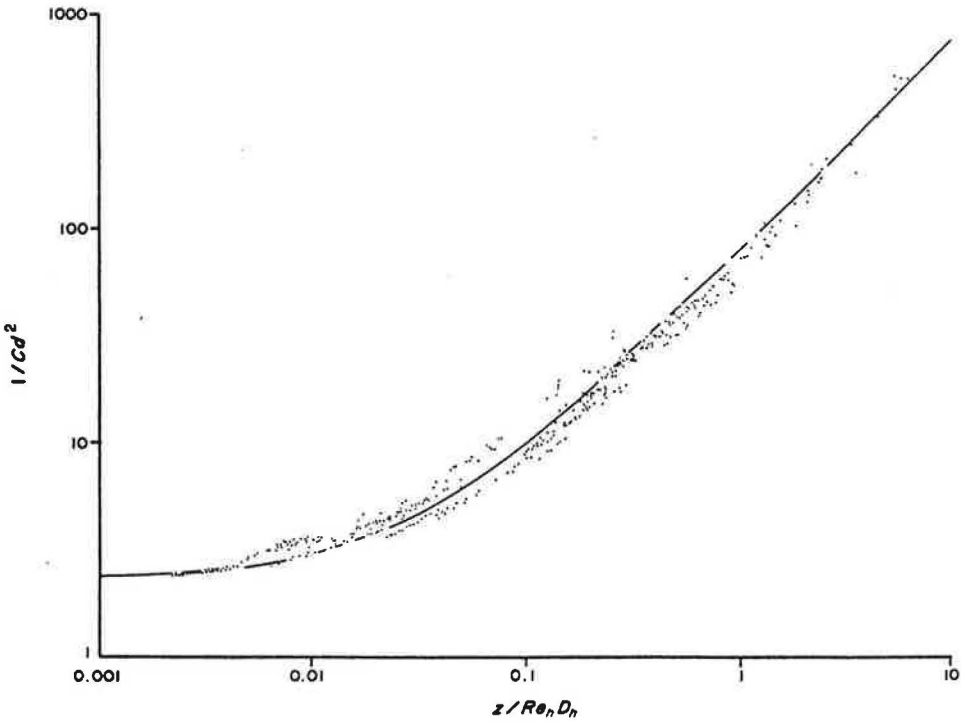

Fig. 5. The relationship between the non-dimensional parameters for flow through L-shaped cracks.

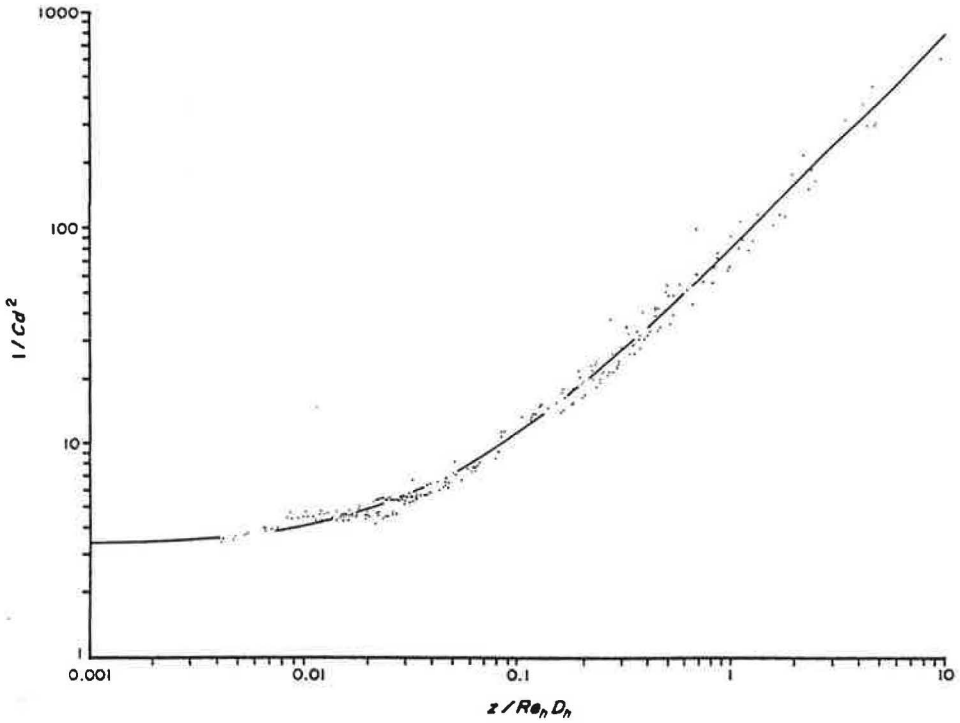

Fig. 6. The relationship between the non-dimensional parameters for flow through double-bend cracks.

gives an intercept of 10.9, yet it is evident from Fig. 4 that as z/Re_hD_h approaches zero, $1/C_d^2$ tends to *ca* 1.5. This poor fit is produced by the disproportionate effect of the greater scatter of data for larger values of the parameters and can be overcome by the selection of a suitable weighting factor in the regression analysis [13].

Weighted least squares analysis produced better linear fits to the data, and the intercepts and slopes thus obtained for the three crack types are compared with the values determined by Etheridge [1] in Table 2.

Although there is good agreement between the values of the intercepts, C, the comparison between the slopes is poor. However, if the 95% prediction intervals for $1/C_d^2$, computed from the data for the present investigation, are drawn through Hopkins and Hansford's experimental results (Fig. 1), then by inspection most of their data fall within the intervals. Thus there is some evidence for agreement between their data and that reported here.

The estimates of the intercepts are close to the predicted values of the loss coefficients for the pressure drop due to bends, assuming that these are the same for flow through parallel plates as for pipe flow [10]: (a) for a combination of a sharp entrance and exit, e.g. crack edges, the loss coefficient, $C = 1.5$ and (b) for a sharp 90° bend, $C = 1$. Thus for a straight-through crack the predicted value of C is 1.5; for a single-bend L-shaped crack, $C = (1.5+1) = 2.5$; and for a double-bend crack, $C = (1.5+1+1) = 3.5$; i.e. $C = 1.5+n_b$, where n_b is the number of bends.

It can be shown (e.g. [1]) that the theoretical relationship for the steady laminar flow through parallel plates is:

$$\frac{1}{C_d^2} = 96 \cdot \frac{z}{D_h} \cdot \frac{1}{Re_h} + C \qquad (11)$$

with the assumption that the total pressure drop across the plates can be considered as the sum of the pressure drops due to skin friction and due to bends and end effects. This relationship was tested against the experimental data for the three crack types, by calculating the percentage deviation (Δ%) of the experimental values of $1/C_d^2$ from those predicted for different values z/Re_hD_h using equation (11). Plots of Δ% vs $z/Re_h \cdot D_h$ are shown in Fig. 7. Equation (11) was considered to be a reasonable approximation to the data if $\Delta\% < \pm 20\%$. For straight-through cracks 82% of the data fulfilled this criterion. However, for L-shaped and double bend cracks, only 48% and 59% of data, respectively, fitted the requirement, although Figs 7b and 7c show that equation (11) is adequate for z/Re_hD_h less than *ca* 0.05.

Figure 7 also shows that the largest deviations from the theoretical relationship were associated with the thinner cracks of each type. Errors in the estimation of the crack thickness may explain the poor fit of the theoretical relationship to the L-shaped and double bend crack data, and the disparities between different workers' estimates of the slopes of the empirical lines through the data (Table 2). For any of the crack models, the 95% Confidence Interval for the mean thickness is about ±0.03

Table 2. Values of the slopes and intercepts of the weighted regression lines (Figs 4–6) for the three crack types and those determined by Etheridge [1] for similar crack geometries

	Present study		After Etheridge [1]	
Crack type	Slope k	Intercept C	Slope k	Intercept C
Straight-through	103.0	1.4	95.7	1.5
L-shaped	78.3	2.3	91.4	2.2
Double bend	78.9	3.3	43.2	3.4

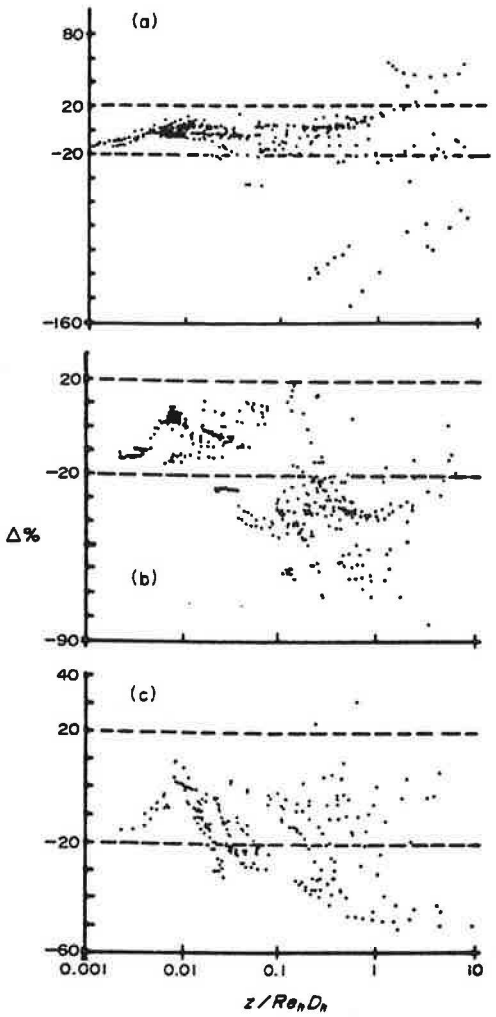

Fig. 7. Fit of the theoretical equation (11) shown as Δ%. (a) Straight-through cracks, (b) L-shaped cracks, (c) double-bend cracks.

m, and the accuracy of each individual measurement is ±0.05 mm. Additionally, unknown errors are introduced for the L-shaped and double bend cracks, since it was not practicable to measure along the complete centre-line of these cracks, e.g. the centre section of the double-bend cracks. Thus a rough estimate of the error in thickness is ±0.1 mm, which is ±10% for a crack of 1 mm thickness, but only ±2% for a 6 mm crack. In the former case the expected errors in the parameters z/Re_hD_h and $1/C_d^2$ are thus ±10% and ±15%, respectively, and for the 6 mm crack ±2% and ±3%. Since data for the thicker cracks ($z/Re_hD_h \to 0$) determine the intercept or loss coefficient, a small error in this may be expected. On the other hand, because the thinner cracks ($z/Re_hD_h \to \infty$) tend to determine the slope of the regression line, the expected error in the slope may be large, e.g. ±27% based on an error of ±10% for a crack thickness of 1 mm.

The above indicates that good agreement between the intercepts determined by the author, by Etheridge's analysis of Hopkins and Hansford's results, and the pseudo-theoretical loss coefficients, may be expected as the error is likely to be small. However, since the error on the slope is likely to be large for a small absolute error in thickness, discrepancies between different workers' estimates of slope are to be expected, particularly for the more complex crack geometries where there is greater uncertainty in thickness measurement, and a poor fit to a theoretical model is also likely.

4.2. *Quadratic solution*

As discussed above, there are reasonable theoretical grounds for describing leakage data with a quadratic equation. Two methods of quadratic analysis were used: (a) curves were fitted to the data using regression analysis; (b) 'theoretical' curves, derived from calculated coefficients, were drawn and compared with the measured data.

4.2.1. *Quadratic regression analysis.* Good quadratic fits were obtained for all data, with a coefficient of determination generally better than 0.99. Some examples are shown in Figs 8–10. The goodness of fit, indicated by inspection of the residuals from the regression analysis and calculation of coefficients of determination, was generally superior, in 61% of the tests, to a power law fit [Figs 8(a) and (b)]. It was considered as good as the power law in 23% of the tests [Fig. 8(c)], whilst the power law was better in 16% of the tests.

The significance of the regression coefficients (Table 3) is best considered by comparison with the theoretical coefficients computed for each crack.

4.2.2. *Theoretical quadratic equations.* The values of the coefficients are,

$$A = 12\mu z/Ld^3 \tag{9}$$

and

$$B = \rho C/2d^2L^2, \tag{10}$$

calculated for each crack, using the measured crack dimensions, experimental ambient conditions, and assuming the loss coefficient, $C = 1.5 + n_b$, are given in Table 3. These were used (i) to construct the theoretical curves as shown in Figs 9 and 10, and (ii) to predict the crack flows at the experimental values of pressure drop, ΔP. The deviation

$$\delta Q\% = \frac{Q_{\text{theory}} - Q}{Q_{\text{theory}}} \times 100\%$$

was then found, which indicates whether the predicted flow, Q_{theory}, under- or overestimates the measured flow, Q.

(i) By inspection, the theoretical curves give a satisfactory fit to most of the data, i.e. well within 20%, which may be taken, arbitrarily, as the limit of acceptability of the theoretical model. (ii) A more rigorous analysis was made by constructing frequency–distribution diagrams with the values of the 'goodness of fit' parameter $\delta Q\%$ for each crack type (Fig. 11). In each case a set of data could be identified which gave a noticeably poorer fit than the majority of the data for that crack type.

It is noteworthy that these data pertain to thinner crack sizes, e.g. 1 mm L-shaped (Fig. 10a) 1 mm double bend, 0.5 mm straight-through (Fig. 10b), which are subject to

Table 3. Experimental (exp) and theoretical (th) values of the coefficients in the quadratic solution

Type	d (mm)	z (mm)	A_{exp}	$A_{th} = 12\mu z/Ld^3$	B_{exp}	$B_{th} = \rho C/2d^2L^2$
S	0.38	152	1130779	1212632	−526679257*	24743767
S	0.90	152	98670	91075	1427614	4370370
S	1.40	152	23346	24063	1808829	1821429
S	3.05	152	2370	2340	366872	382155
S	6.15	152	338	285	83851	94785
S	9.40	152	121	80	34741	40403
S	8.94	76	93	46	36431	45644
S	5.85	76	291	166	84435	106421
S	2.85	76	1722	1435	429895	445799
S	1.39	76	13494	12373	1160443	1869468
S	1.03	76	33854	30446	−1520483*	3339617
S	0.55	76	99680	199242	907575	11920661
S	0.49	50	257262	185331	1107877408	14693878
S	1.17	50	12324	13579	1882549	2567144
S	1.79	50	3661	3841	1061599	1102121
S	3.20	50	708	666	334264	341602
S	6.08	50	162	97	75335	94951
S	9.13	50	53	29	34646	41748
LE	6.00	94	128	190	190024	162500
LE	2.98	96.02	1541	1585	662393	664384
LE	1.09	98.91	25660	33545	264683	4965912
LUS	5.99	64.01	173	130	231323	163043
LUL	„	„	186	„	137704	„
LUS	3.10	66.90	1147	981	627699	613944
LUL	„	„	1048	„	504660	„
LUS/L	1.08	68.92	17255	23898	4133307	5058299
DS	3.16	150	956	2088	890830	820181
DS	1.09	150	38288	50594	7274357	6834442
DS	3.14	60	1501	844	677975	851962
DS	1.09	60	10251	20237	8461119	7040653
DU	3.23	143.53	1345	1852	805036	796285

S, Straight through; LE, L-shaped equal 50 mm × 50 mm sections; LU, L-shaped unequal 20 mm × 50 mm (S = short exit, L = long exit); DS, double bend 'S'; DU, double bend 'U'.
* The negative values of B_{exp} are a consequence of the spread of data.

greater proportional, dimensional errors than the thicker cracks. It can readily be shown, when deriving the theoretical coefficients, if the absolute dimensional error is taken as 0.1 mm, that this is sufficient to cause errors of approximately ±25% in the coefficients predicted for a small crack thickness, but for thicker cracks these errors become less significant (~ ±5%). There was therefore reasonable justification for rejecting these data from the analyses of the distributions (Table 4).

For the theory to be acceptable the mean value of $\delta Q\%$ should be zero, but using a rigorous statistical treatment of the $\delta Q\%$ values the actual mean value of −3.1% can be shown to be significant, so the model should be rejected. However, it can also be shown that the mean $\delta Q\%$ is significantly less than ±5%, which is an acceptable prediction error limit for a model. Also, since greater than 90% of the data fall within the ±20% acceptance limits for individual datum points, there is reasonable evidence for accepting the theoretical quadratic model.

The model is sufficiently accurate for it to be considered as a rule of thumb method for estimating, for example, leakage areas using pressure drop-flow measurements. However, an accurate solution may be difficult to achieve, since once a leakage path has been identified, it is unlikely that its critical dimensional characteristics (thickness, centre-line distance and number of bends) are either known or practically measurable, unless the path is formed by a building component such as a door. The parameters which can be easily obtained from simple measurements are crack length, and air density and viscosity, from ambient conditions. Using a pressure box technique, crack length is fixed at a predetermined value,

Table 4. Analyses of frequency–distributions of the deviations. $\delta Q\%$

Crack type	Sample size	Mean $Q\%$	Standard deviation	95% Confidence original of mean	Goodness of fit: % of data within acceptance limits
Straight-through	281	−1.3	10.8	1.3	95
L-shaped	325	−2.8	13.2	1.5	87
Double bend	151	−7.3	7.5	1.2	97
All	757	−3.1	11.5	0.8	92

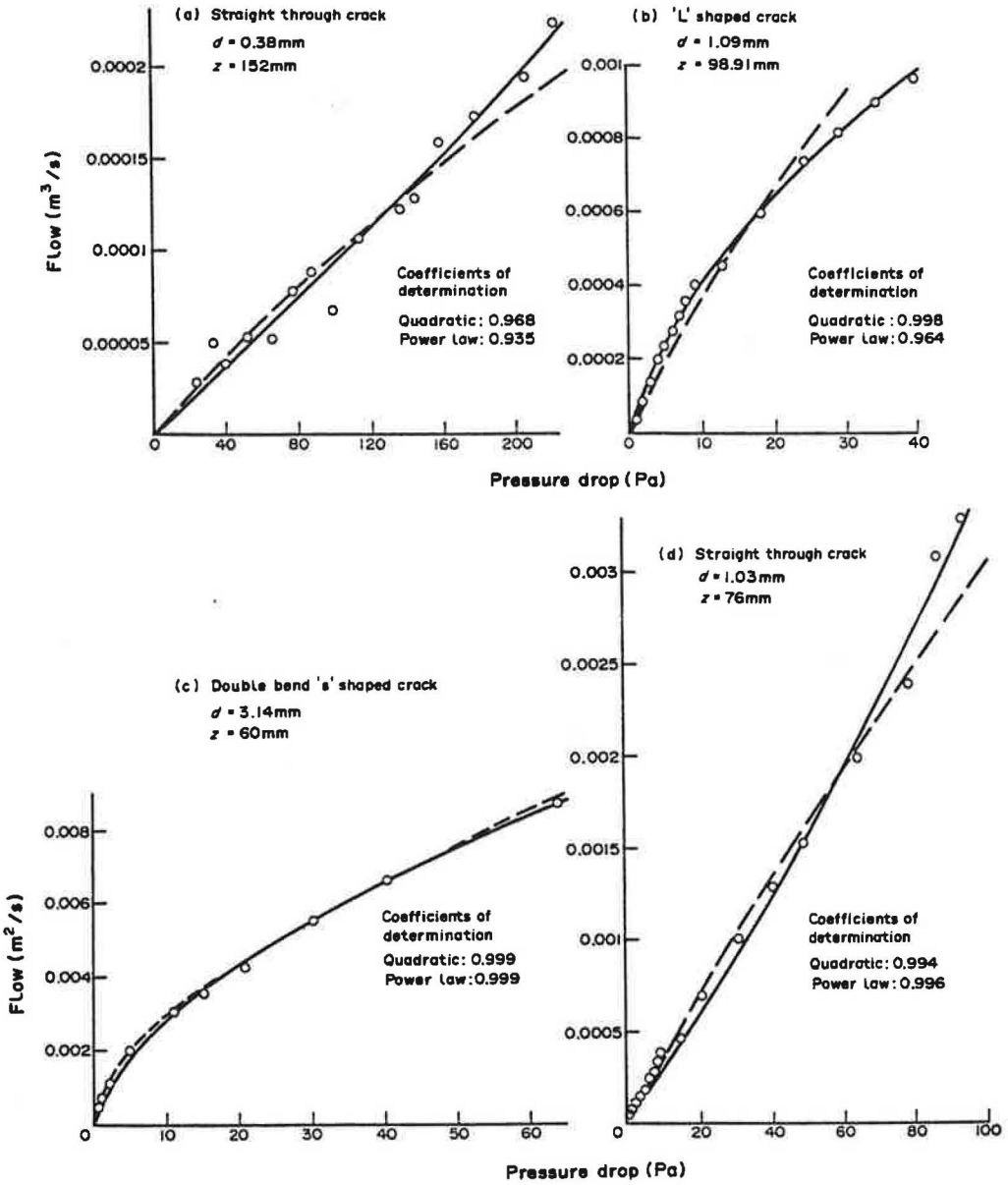

Fig. 8. Examples of this quadratic and power law fits: (a) and (b) quadratic better than power law, (c) quadratic as good as power law, (d) power law better than quadratic.

say 0.5 m as in this investigation, and then the flow through the complete crack is found pro-rata. The experimental values of the quadratic coefficients, A and B, can then be substituted along with other known crack parameters into equations (9) and (10), which can be rearranged to give the unknown parameters on the left:

$$\frac{z}{d^3} = \frac{AL}{12\mu}$$

and

$$\frac{C}{d^2} = \frac{2BL^2}{\rho}.$$

An exact solution for leakage area, defined as the product Ld, cannot be found, since there are three unknowns and only two equations, but a good estimate may be obtained by a graphical method. Figure 12 shows bands constructed for 0.5 m long cracks of various thicknesses, 0.5–9 mm, at 20°C. The curves which form the limits (z = 50–150 mm) were drawn using the quadratic model (equation 6).

Experimental flow pressure drop measurements are plotted onto the diagram. The approximate crack thickness can then be read off. Shown are some data measured for L-shaped cracks. The method works well for the cracks with nominal thicknesses of 1 and 3 mm, since there is reasonable differentiation between the bands. However, for thicknesses greater than about 3 mm, the bands overlap considerably, thus for the 6 mm L-shaped cracks the best estimate of thickness is 5–7 mm. For more

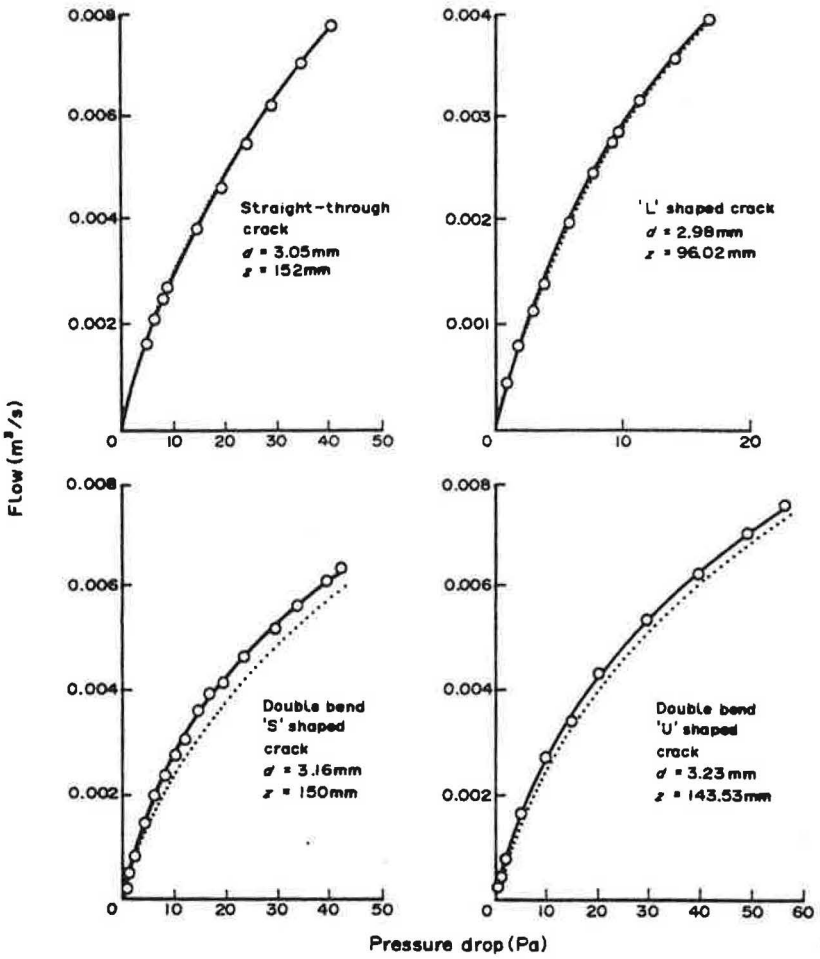

Fig. 9. Typical flow characteristic curves, ——— quadratic regression fit to experimental data, ... theoretical relationship:

$$\Delta P = \frac{12\mu Z}{d^3 L} Q + \frac{C\rho}{2d^2 L^2} Q^2.$$

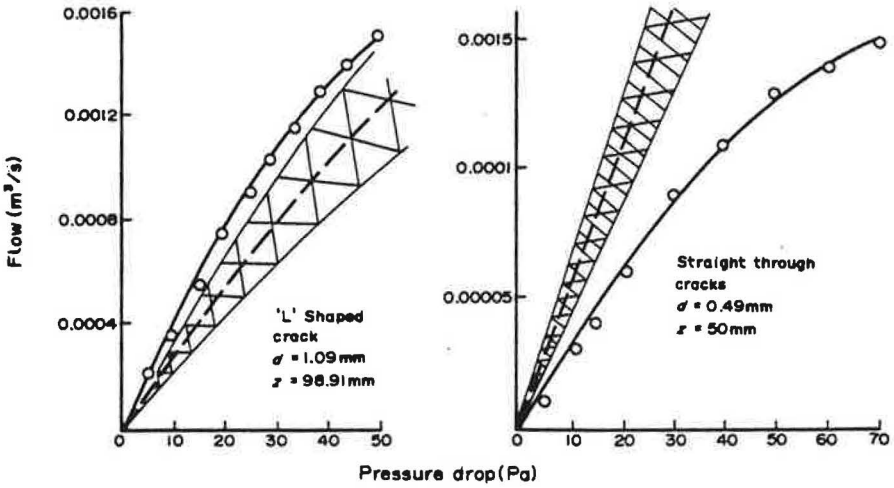

Fig. 10. Examples of poor fit of the theoretical relationship to the data. Hatched areas represent ±20% acceptability limits.

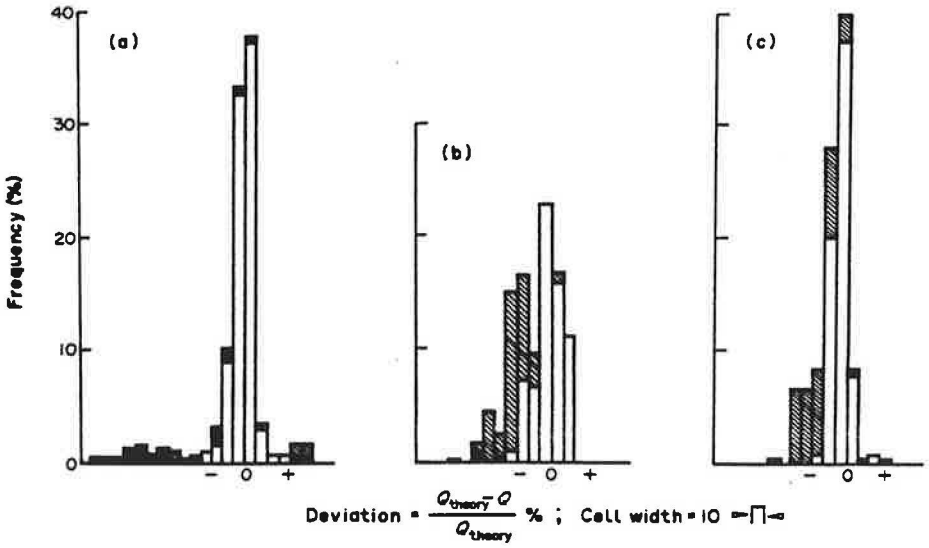

Fig. 11. Distribution of deviations, (a) straight-through cracks, (b) L-shaped cracks, (c) double bend cracks. Shaded areas refer to rejected data.

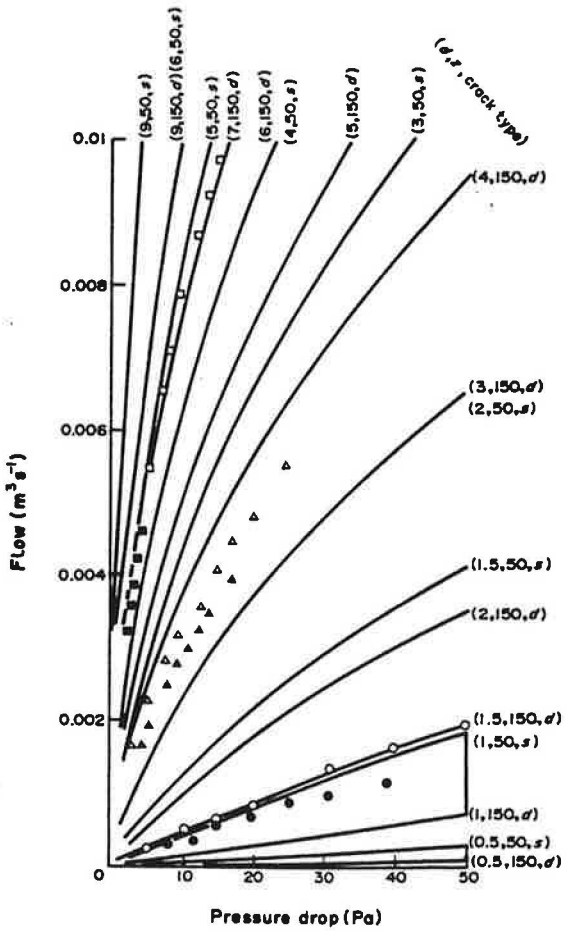

complex cracks and values of z outside the range of the diagram, the method gives an apparent crack thickness.

4.3. *Conclusions*

(1) The relationship:

$$\frac{1}{C_d^2} = k \cdot \frac{k}{D_h} \cdot \frac{1}{Re_h} + C \tag{8}$$

adequately describes crack flow for a wide range of the parameter z/Re_hD_h. However, agreement with the experimental data deteriorates at higher values of z/Re_hD_h.

(2) The intercept or loss coefficient C in equation (8) approximates to $(1.5+n_b)$, where n_b is the number of bends. This estimate can be used in theoretical quadratic equations (see 4 below).

(3) A quadratic curve of the form:

$$\Delta P = A \cdot Q + B \cdot Q^2$$

describes the experimental data better than a power law, $\Delta P = \alpha Q^{\beta}$.

Fig. 12. Flow characteristic chart: Curves drawn for various crack types (d mm, z mm, crack type: s = straight-through; d = double-bend). Experimental Data:

L-shaped cracks	d mm	z mm
□	6	
△	3	70
○	1	
■	6	
▲	3	100
●	1	

(4) A theoretical quadratic model of crack flow

$$\Delta P = \frac{12\mu z}{Ld^3} \cdot Q + \frac{\rho C}{2d^2L^2} \cdot Q^2 \qquad (6)$$

obtained from the same parallel plate theory as equation (8), is suggested as a more practical alternative to the more general non-dimensional solutions found in equation (8), since adequate estimates of the parameters

$$A = \frac{12\mu z}{Ld^3} \quad \text{and} \quad B = \frac{\rho C}{2d^2L^2}$$

can be readily obtained by quadratic regression analysis of the experimental data.

(5) Both the quadratic model, equation (6), and the non-dimensional solution, equation (8), can be used to produce a simple graphical method of predicting crackage areas from measured data based on a known crack length.

Acknowledgement—The work described in this note was funded by a research grant from the Science and Engineering Research Council (Grant No. GR/C51363).

REFERENCES

1. D. W. Etheridge, Crack flow equations and scale effect. *Bldg Envir.* **12**, 181–189 (1977).
2. J. B. Dick, The fundamentals of natural ventilation in houses. *JIHVE* **18**, 123–134 (1950).
3. M. H. Sherman, D. T. Grimsrud and R. C. Sonderegger, Low pressure leakage function of a building. *Lawrence Berkeley Lab. Report* LBL-9162 (1979).
4. L. P. Hopkins and B. Hansford, Air flow through cracks. *Build. Serv. Engr.* **42**, 123–129 (1974).
5. D. A. Thomas and J. B. Dick, Air infiltration through gaps around windows. *JIHVE* **21**, 85–97 (1953).
6. M. S. Jones, Discussion of J. B. Dick's experimental studies in natural ventilation of houses. *JIHVE* 462, 463 (Dec. 1949).
7. D. W. Etheridge, Air leakage characteristics of houses: a new approach. *Build. Serv. Engr. Res. Tech.* 5, 32–36 (1984).
8. R. W. Fox and A. T. MacDonald, Introduction to fluid mechanics, 2nd ed. Wiley, New York (1978).
9. BS 1042: Part R: Methods for the measurement of fluid flow in pipes; orifice plates, nozzles and venturi tubes (1964).
10. E. Ower and R. C. Pankhurst, The measurement of air flow, 5th ed. Pergamon, Oxford (1977).
11. BS 1042 1 Section 2.1: Measurement of fluid flow in closed conduits, Method using Pitot Static Tubes, BSI (1983).
12. P. H. Baker, S. Sharples and I. C. Ward, Air flow through asymmetric building cracks. *Build. Serv. Engr. Res. Tech.* 7, 107–108 (1986).
13. P. H. Baker, S. Sharples and I. C. Ward, BS 82, Department of Building Science, Sheffield University, Internal Report (1987).